Use of a quantitative index of beam modulation to characterize dose conformality: illustration by a comparison of full beamlet IMRT, few-segment IMRT (fsIMRT) and conformal unmodulated radiotherapy

2003 Phys. Med. Biol. 48 2051

(http://iopscience.iop.org/0031-9155/48/14/301)

INSTITUTE OF PHYSICS PUBLISHING PHYSICS IN MEDICINE AND BIOLOGY

Phys. Med. Biol. **48** (2003) 2051–2062 PII: S0031-9155(03)61630-1

Use of a quantitative index of beam modulation to characterize dose conformality: illustration by a comparison of full beamlet IMRT, few-segment IMRT (fsIMRT) and conformal unmodulated radiotherapy

S Webb

Joint Department of Physics, Institute of Cancer Research and Royal Marsden NHS Trust, Downs Road, Sutton, Surrey, SM2 5PT, UK

Received 2 April 2003
Published 1 July 2003
Online at stacks.iop.org/PMB/48/2051

Abstract

A technique is presented for characterizing the degree of modulation in an intensity-modulated beam. It is shown that the modulation increases as dose conformality increases. Full intensity-modulated radiation therapy (IMRT) is compared with a two-weight-per-field technique and with simple geometrically conformal beams. It is suggested that each individual planning problem requires some comparative planning of this type because there is no simple answer to the question of the degree to which IMRT improves dose conformality. This depends on the problem geometry, the dose prescription, the cost function, the number of beams and other planning conditions. A methodology is presented for such comparative planning studies and this is illustrated with the solution of two planning problems.

1. Introduction

Intensity-modulated radiation therapy (IMRT) exploits the ability to combine fluence-modulated beams to create high-dose volumes with many advantages over those that may be created using geometrically conformal beams without fluence modulation. These advantages include potentially: (i) the creation of contorted isodose contours which can 'shrink-wrap' the high dose on to concave volumes, (ii) the ability to paint different doses to different parts of the planning target volume (PTV) if this is indicated (e.g., through imaging studies), (iii) superior shielding of organs at risk. Methods for planning and delivery are now well established and in clinical use (Webb 2000).

Somewhere between the two extremes of zero-modulation (geometrically) conformal radiotherapy (CRT) and allowing beam-element (bixel) values to fully vary lie the techniques of using a few static segments from each direction. Several groups are developing techniques to plan the weights of such segments by forward rather than inverse planning. The ideas of

both few-segment fields and forward planning are intrinsically attractive, representing both a small paradigm shift from (geometrically) conformal therapy and the possibility for simpler delivery.

Somewhat inevitably, given the rapid growth of the technology of IMRT and currently limited data on its clinical benefit, there has been something of a backlash against the overenthusiasm for the field (Schulz and Kagan 2002) and also a reawakening of interest in the question of whether few-segment IMRT (fsIMRT) can 'do as well'. Fundamentally it must be true that it cannot, given that removing degrees of freedom from the inversion problem of determining bixel beam weights from dose prescription must reduce the ability to conform the dose. However, this is not in itself the difficulty. The real difficulty lies in understanding the fundamental relationship between the delivered dose and the field configurations required to obtain it. There is a need for some clear 'index of modulation' to describe the variability of bixel values in a beam and, moreover, a need to be able to relate this to the degree of dose conformality. In this paper dose conformality has been characterized numerically by the ratio of the mean dose to organs at risk and the mean dose to the planning target volume, 'good conformality' being a low ratio. Also the conformality has been quantitated by tabulating other dose statistics such as the minimum and maximum doses to these regions as well as visual inspection of isodose plots. Whilst there have been a large number of modelling studies showing specific dose distributions and their corresponding beam fluence modulations, there is less written about the comparative planning of test situations with CRT, fsIMRT and IMRT. Shepard *et al* (1999) have provided the only known comparison. The aim of this paper is to cast some light on this problem and make some proposals and observations concerning quantifying the above relationships.

At the outset it must be said that this is a near impossible task to study in its entirety given that the achieved dose distribution depends not only on the prescription but also on the constraints set on the problem, the form of the cost function, the value set for importance weights, the variable number of fields, the variable type of prescription with its degree of concavity and the number and juxtaposition of organs at risk. In short it is suggested that there is no single answer to the question 'do we need IMRT?'. More usefully the paper establishes some basic tests that can be undertaken to describe the ranking of approaches to any particular planning problem. A study by Hunt *et al* (2002) showed that the modulation can be related to the importance factors and gave a protocol for inverse planning. That study did not investigate the asymptotic limit of fsIMRT and CRT. Coolens *et al* (2003) studied the dependence of conformality on the systematic substitution of some intensity-modulated beams with geometrically conformal beams and characterized the residual modulation. The present study is different from this but complements it.

2. Method

2.1. Establishing a measure of modulation

For simplicity, consider planning a 2D slice of a patient using a series of 1D fields. Let the kth beam at some orientation have n sequential elements of bixel intensity I_p, $p = 1, 2, 3, \ldots, n$. Calculate the mean ($\langle I \rangle$) and standard deviation σ_I of these values. Let $\Delta_p = \mathrm{abs}(I_p - I_{p-1})$ ($p = 2, 3, \ldots, n$) be the magnitude of the difference between the intensity I_p of the pth bixel and the intensity I_{p-1} of the $(p-1)$th bixel. Now count the number $N(f; \Delta_p > f\sigma_I)$ of changes for which $\Delta_p > f\sigma_I$ where $f = 0.01, 0.02 \ldots 2$ and hence the fraction $z(f)$ of such changes of all changes in the beam, i.e. $z(f) = \left(\frac{1}{(n-1)}\right) N(f; \Delta_p > f\sigma_I)$. The function $z(f)$ is a spectrum of the number of adjacent-element changes that exceed a certain fraction of the

standard deviation in the beam. It always falls monotonically as f increases. The area under the spectrum is an indication of the degree of modulation and $\mathrm{MI} = \int_0^{0.5\sigma} z(f')\,\mathrm{d}f'$ has been chosen as a single numerical measure of the modulation, christened the 'modulation index' (MI). Some example modulations will be shown from which it will be clear that this integral increases as the variability (modulation) of the beam increases. Llacer *et al* (2001) proposed an alternative 'fluence map complexity (FMC)' measure which was a normalized root sum over the local differences between bixel values and their two neighbours. This FMC also increases with increased modulation (decreased smoothness) though it acts locally rather than relates local changes to the overall beam property of standard deviation. It responds well to individually high or low bixels relative to nearest neighbours.

It should be emphasized that these measures of beam modulation compute the degree of modulation *a posteriori*. The new measure is not used here to *control* the degree of modulation. However, in principle it could be incorporated into some cost function as a measure of control. Webb (2001) has previously presented a technique for optimizing IMRT based on a cost function which combines a measure of the conformality in dose space and the smoothness in beam space.

The MI is a better measure of beam structure than the standard deviation itself because it quantitates the variations between adjacent bixel intensities and it is these which determine the degree of difficulty some MLC-based delivery systems have. For example, a beam of ten bixel intensities (1, 2, 1, 2, 1, 2, 1, 2, 1, 2) and another with ten intensities (1, 1, 1, 1, 1, 2, 2, 2, 2, 2) have the same means and standard deviations, but the former is more modulated and would have a larger value of MI and be more difficult to deliver.

2.2. Comparative planning

The aim was to illustrate the use of the MI by making some comparisons of CRT, fsIMRT and IMRT for the same planning problems and with as many potential variables set to be common between the three situations. This should overcome concerns that comparing studies between different papers does not investigate standardized configurations. Each planning case was specified on a 2D dose grid of $(i = 64) \times (j = 64)$ pixels of size 0.25 cm^2. The planning target volume (PTV) and organs at risk (OAR) and rest of body (ROB) contours were specified. The dose prescription $D^p_{i,j}$ to each of these was specified together with the importance factors $wt_{i,j}$ in a quadratic cost function, $\mathrm{cost} = \sum_{i=1}^{64}\sum_{j=1}^{64} wt_{i,j}\left(D^p_{i,j} - D^c_{i,j}\right)^2$, where $D^c_{i,j}$ is the computed dose distribution. A downhill optimization algorithm minimized this cost iteratively. 10^6 iterations were performed taking about 6 min on a COMPAQ Alphastation 250/4 266 computer. The 1D beams, which each had 64 elements with a bixel size of 0.5 cm, were arranged equispaced in 0–2π. A simple dose model, dose = bixel weight $\times \exp(-\mu \times \mathrm{depth})$, was used with $\mu = 0.04$ cm^{-1}. Beam positivity was ensured by rejecting any changes that would have made a bixel value negative. The dose prescription and the importance weights varied between the problems studied. The importance factors for the IMRT situation were adjusted through experiment until the dose distribution in the PTV was considered acceptable and then these same parameters were used for the corresponding fsIMRT and CRT situations.

Three versions of the code were implemented. In the first (modelling IMRT) the bixels could fully vary independently. The optimization code randomly polled beam angles and bixels, added grains of beam weight, computed the iteratively changing dose distribution, and accepted or rejected these changes depending on whether the cost function decreased or increased. Fully modulated (i.e. all bixels can vary independently) intensity-modulated beams (IMBs) resulted. These showed the expected peaks and troughs obtainable with full bixel modulation but did not exhibit unwanted noise. In the second code (modelling a simple form

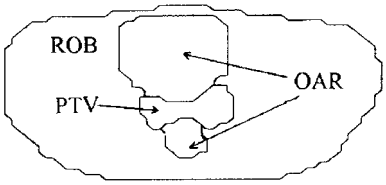

Figure 1. The first representative planning slice showing the PTV, OAR and ROB contours (not to scale).

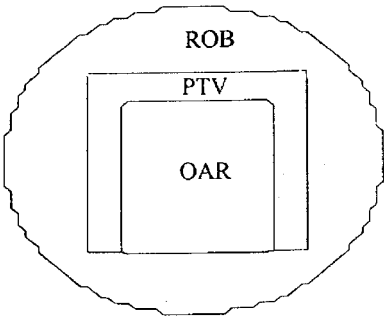

Figure 2. The second representative planning slice showing the PTV, OAR and ROB contours (not to scale).

of fsIMRT) the beams were each split into two segments, one with a beam's-eye-view (BEV) of that part of the PTV which excludes the simultaneous BEV of the OAR and the other with a BEV of that part of the PTV which includes the simultaneous BEV of the OAR (Webb 1991, Mohan *et al* 1992, Bos *et al* 1999). The two-segment-per-beam weights were independently optimized. In the third code (representing CRT) the beams connected to just PTV with a single weight for each beam.

The outcomes of the planning were assessed in several ways. Firstly the mean, minimum and maximum dose to PTV, OAR and ROB were scored throughout and at the termination of the iterative cycles. Dose distributions and profiles of the bixel values were plotted and inspected. Thirdly the beam spectra were computed and the mean value (simple average over the number of beams) of the modulation index was found, representing the 'degree of modulation' of the beams.

The first case studied was to plan on the PTV and OARs in a slice of the case reported by Bortfeld *et al* (1994) which was used as the first application of IMRT with a MLC. The slice and its contours are shown in figure 1. The dose prescription was set to be PTV:OAR:ROB = 100:30:30 and the importance weights were set to be wt_{PTV}:wt_{OAR}:wt_{ROB} = 20:1:0.5 for both five-field and nine-field situations. Subsequently the nine-field situation was replanned with dose prescription PTV:OAR:ROB = 100:0:0 and the importance weights were set to be wt_{PTV}:wt_{OAR}:wt_{ROB} = 70:1:0.5.

The second case studied was the attempt to create a right-angled horseshoe PTV with an OAR in its cusp, with these structures inside a circular body section of radius 28 cm (figure 2). This represents the classic 'tough problem' for treatment planning. The dose prescription was set to be PTV:OAR:ROB = 100:0:0 and the importance weights were set to be wt_{PTV}:wt_{OAR}:wt_{ROB} = 10:0.1:0.5 for the four-field and wt_{PTV}:wt_{OAR}:wt_{ROB} = 50:0.1:0.5 for the nine-field situations. For all situations beam angles were uniformly spaced in 2π.

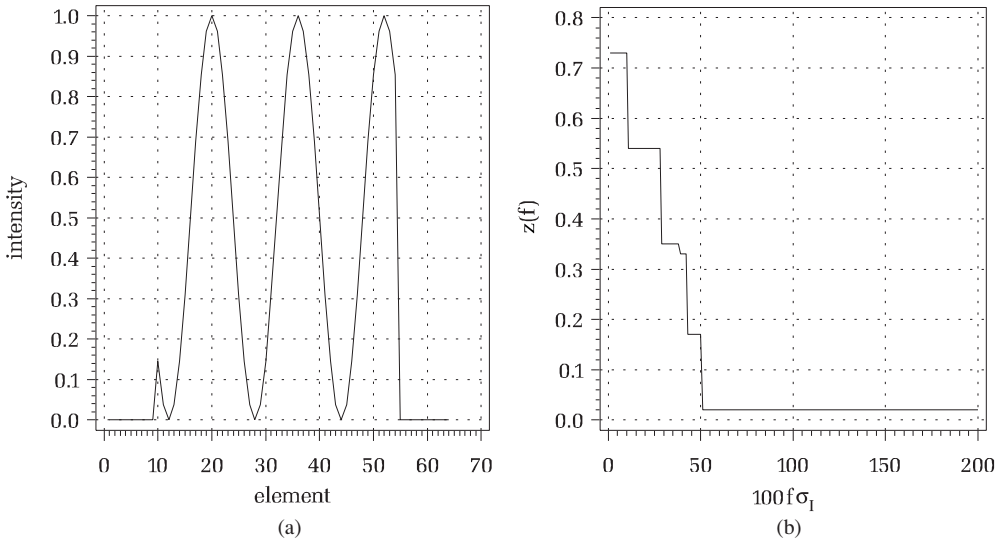

Figure 3. (a) A 1D intensity-modulated beam and (b) its spectrum.

Table 1. The modulation index, $\mathrm{MI} = \int_0^{0.5\sigma} z(f')\,\mathrm{d}f'$, for test 1D modulations.

Type of 1D modulation	Modulation index
Double-step function: value of 0.3 between elements 10 and 30; value of 1 between elements 31 and 55; elsewhere zero	2.381
Simple ramp from 0 to 1 between beam elements 10 and 55	4.984
Sinewave of periodicity 64 bixels	5.444
Sinewave of periodicity 16 bixels	23.238
Sinewave of periodicity 8 bixels	31.524
Sinewave of periodicity 4 bixels	36.508
Random values in the range 0–1 between elements 10 and 55; zero elsewhere	28.619

3. Results

3.1. Measures of modulation

Table 1 shows the value of the integral in section 2.1, the modulation index, for a variety of specified test modulations in a 1D IMB. Note that as the modulations become more complex so the value of this modulation index increases. An example modulated IMB and its spectrum are shown in figures 3(a) and (b).

3.2. Comparative planning

Table 2 shows the statistics for the three types of planning on the first model slice. Figures 4(a)–(c) and 5(a)–(c) show the corresponding dose distributions for the upper two panels in the table. The IMBs and spectra are not shown since they would show confusing detail. However, the

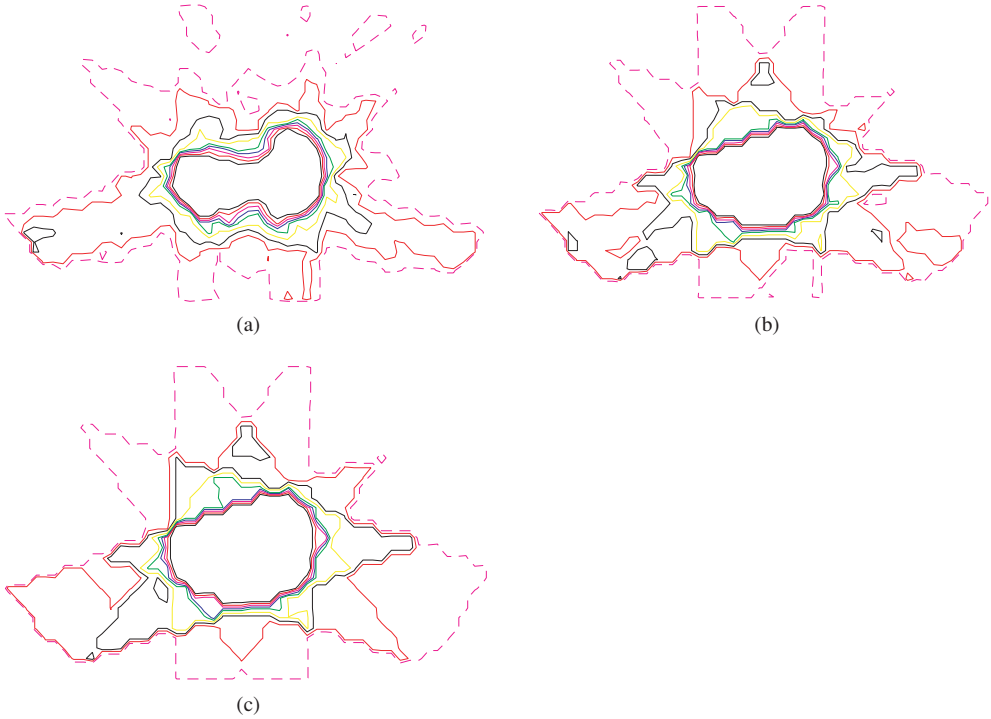

Figure 4. (a) Dosemap from IMRT, (b) dosemap from fsIMRT and (c) dosemap from CRT (prostate-model; five beams). The mean dose in the PTV has been normalized to 100 so the isodoses shown are the 90% (black), 85% (red), 80% (purple), 75% (blue), 70% (green), 60% (yellow), 50% (black), 40% (red), 30% (red dotted).

Table 2. Dose statistics for three types of planning (problem 1).

	IMRT			fsIMRT			CRT		
	mean	min	max	mean	min	max	mean	min	max
Prostate-model problem (Dose prescription: PTV:OAR:ROB = 100:30:30)									
Five equispaced beams									
PTV	98.34	88.79	105.87	97.29	91.32	103.28	97.08	95.51	99.19
OAR	37.25	1.63	92.07	44.56	10.43	95.12	45.83	11.14	100.21
ROB	25.43	0	94.77	27.14	0	99.68	27.49	0	99.39
MI		7.778			2.333			1.587	
Nine equispaced beams									
PTV	99.25	94.26	103.63	97.70	90.88	106.52	97.44	96.19	99.50
OAR	33.73	12.06	86.22	42.93	15.93	91.92	44.39	15.48	98.88
ROB	25.42	0	89.20	28.82	0	96.98	29.37	0	99.04
MI		8.624			2.439			1.587	
Prostate-model problem (Dose prescription: PTV:OAR:ROB = 100:0:0)									
Nine equispaced beams									
PTV	98.86	93.20	104.92	99.02	96.84	101.42	99.00	97.97	100.38
OAR	22.93	0	85.80	61.58	30.64	98.35	61.66	30.25	100.24
ROB	22.69	0	90.12	22.90	0	99.35	23.04	0	100.28
MI		7.991			2.113			1.587	

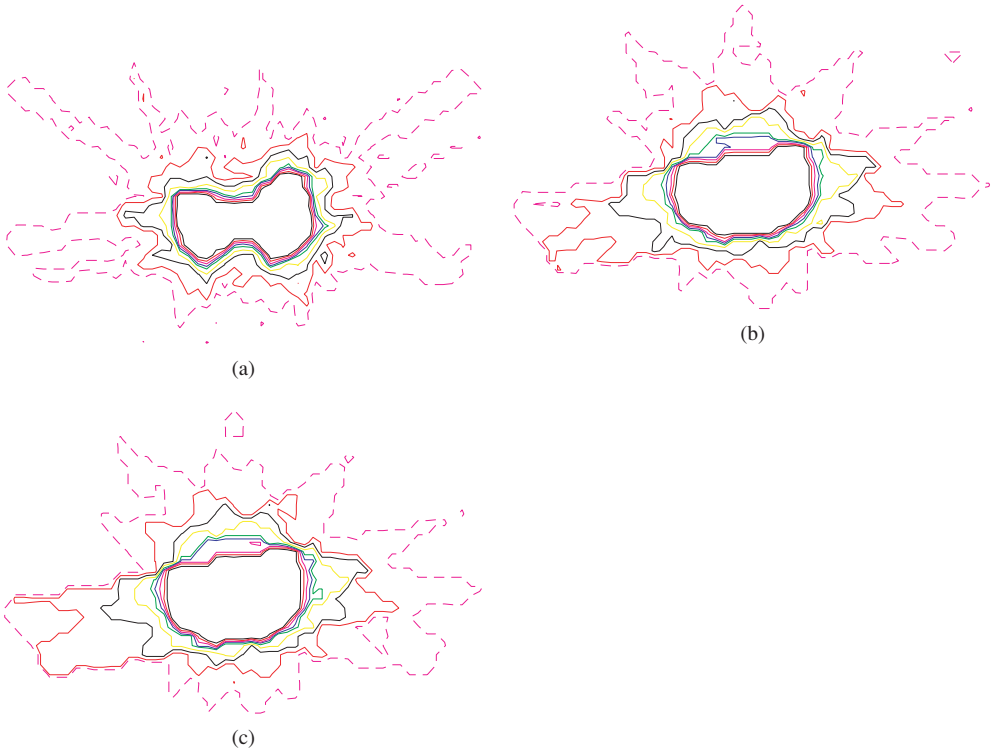

Figure 5. (a) Dosemap from IMRT, (b) dosemap from fsIMRT and (c) dosemap from CRT (prostate model: nine beams). The mean dose in the PTV has been normalized to 100 so the isodoses shown are the 90% (black), 85% (red), 80% (purple), 75% (blue), 70% (green), 60% (yellow), 50% (black), 40% (red), 30% (red dotted).

Table 3. Dose statistics for three types of planning (problem 2).

	IMRT			fsIMRT			CRT		
	mean	min	max	mean	min	max	mean	min	max
Horseshoe-model problem (Dose prescription: PTV:OAR:ROB = 100:0:0)									
Four equispaced beams									
PTV	97.01	90.50	111.25	96.65	87.75	113.95	95.74	90.96	105.16
OAR	53.06	30.56	75.16	61.09	56.20	70.92	90.93	88.19	96.42
ROB	36.09	0	104.87	38.19	0	78.90	46.93	0	56.81
MI		3.762			2.778			1.587	
Nine equispaced beams									
PTV	99.54	89.41	107.52	98.68	87.81	106.63	98.52	94.04	107.48
OAR	36.62	0.24	94.59	87.23	84.21	93.90	94.39	91.19	102.68
ROB	38.41	0.50	106.05	60.47	32.82	106.63	64.86	25.29	107.58
MI		12.340			1.965			0.882	

mean value of the modulation index is given (averaged over the m beams). We may observe:

(i) The mean value to the PTV edges closer to the prescription 100 as the planning complexity increases from CRT to fsIMRT to IMRT, irrespective of the number of contributing beams;

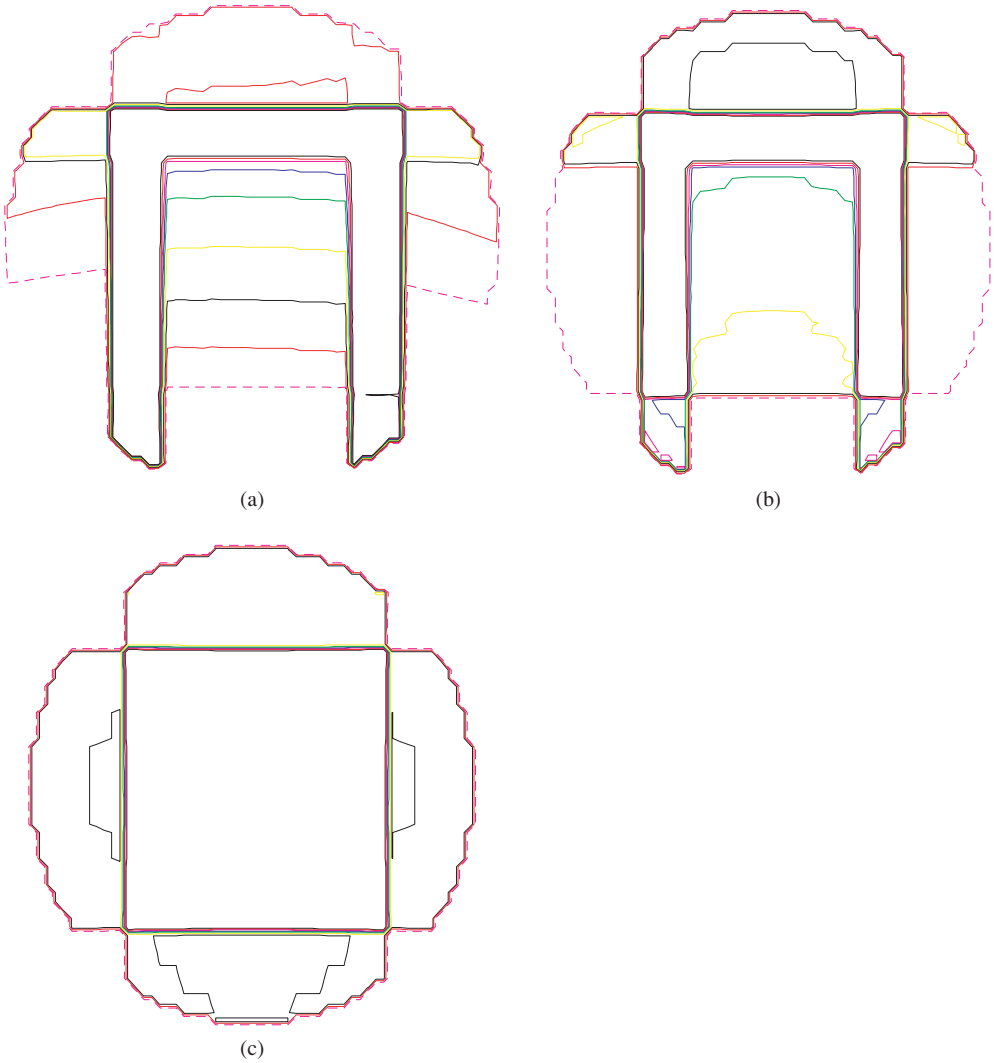

Figure 6. (a) Dosemap from IMRT, (b) dosemap from fsIMRT and (c) dosemap from CRT (horseshoe model: four beams). The mean dose in the PTV has been normalized to 100 so the isodoses shown are the 90% (black), 85% (red), 80% (purple), 75% (blue), 70% (green), 60% (yellow), 50% (black), 40% (red), 30% (red dotted).

(ii) For any specified type of planning the mean PTV dose improves when the number of beams is increased from 5 to 9;
(iii) The protection of the OAR improves (lower mean, min and max) as the planning complexity increases from CRT to fsIMRT to IMRT;
(iv) For any specified type of planning the mean OAR dose decreases as the number of beams increases;
(v) The increased conformality correlates with increased value of the modulation index.

Table 3 shows the statistics for the three types of planning on the horseshoe problem. Figures 6(a)–(c) and 7(a)–(c) show the corresponding dose distributions. Note that for the

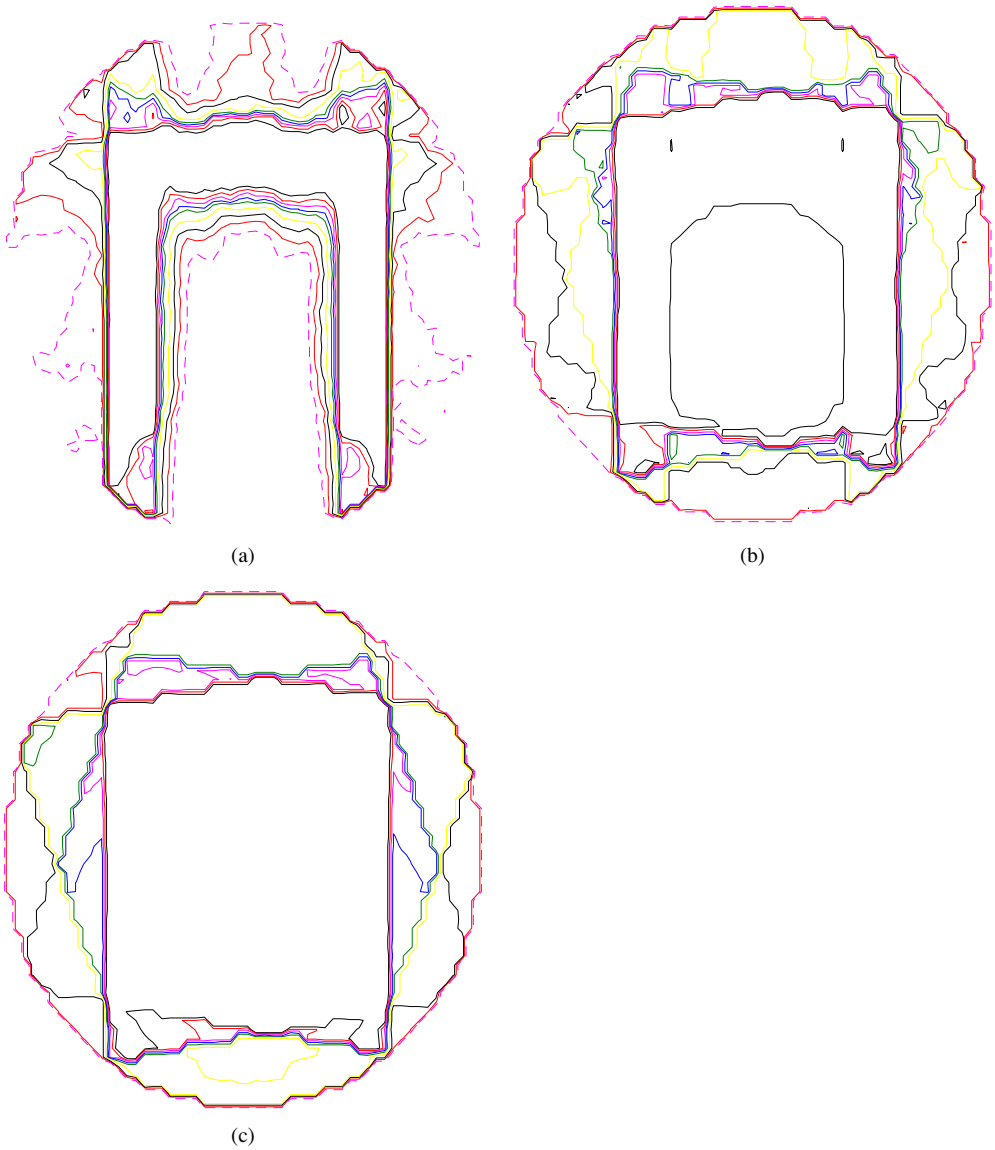

Figure 7. (a) Dosemap from IMRT, (b) dosemap from fsIMRT and (c) dosemap from CRT (horseshoe model: nine beams). The mean dose in the PTV has been normalized to 100 so the isodoses shown are the 90% (black), 85% (red), 80% (purple), 75% (blue), 70% (green), 60% (yellow), 50% (black), 40% (red), 30% (red dotted).

four-beam case the beams entered along the principal directions of the horseshoe and this gives the configuration an atypical advantage in determining conformality. We know from the study of Bortfeld and Schlegel (1993) that beam angle optimization will tend to select angles that are geometrically favourable with respect to predominant edges in targets (e.g., ask an algorithm to pick the 'good directions' for four beams to irradiate a box and they will align with the box-edge directions). When nine fields are used for IMRT the conformality is excellent. When nine fields are used for fsIMRT the result is worse than for four-field CRT.

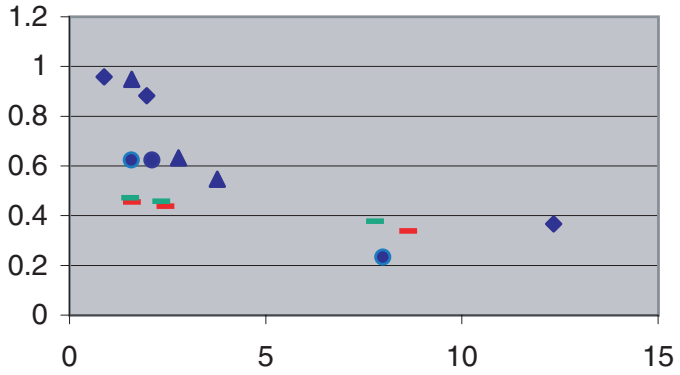

Figure 8. The ratio of the mean dose in OAR to the mean dose in PTV (vertical axis) as a function of the value of the mean value of the modulation index (horizontal axis). key: diamonds = horseshoe shape problem (nine fields); triangles = horseshoe shape problem (four fields), red line = prostate problem (nine fields), dose prescription PTV:OAR:ROB = 100:30:30; green line = prostate problem (five fields), dose prescription PTV:OAR:ROB = 100:30:30; blue circles = prostate problem (nine fields), dose prescription PTV:OAR:ROB = 100:0:0.

All the conclusions listed above ((i) to (v)) for the prostate model were replicated for the horseshoe model, specifically that conformality increases from CRT through fsIMRT to IMRT with corresponding increases in the beam modulation index.

Figure 8 shows a plot of the ratio of the mean dose in the OAR to the mean dose in the PTV (characterizing dose conformality) as a function of the value of the mean of the modulation index. As commented above the monotonic relationship between these parameters is evident. Conformality increases as the mean of the modulation index increases. However, the data points do not lie on a *single* curve. This emphasizes that the degree of conformality that can be obtained with a specific modulation must depend on the geometry of the problem being tackled and on the dose prescription and importance factors. Put the other way round 'some geometries need IMRT more than others'.

4. Discussion and conclusions

It is not surprising to have found that permitting full modulation of bixels leads to better dose conformality than the fsIMRT technique and in turn the CRT technique, this being the fundamental rationale behind the development of IMRT. This paper has investigated the relationship between the three planning methods whilst keeping constant the other planning conditions (same dose model, same geometry, same number of beams, same dose prescription, same importance factors, etc). This allows a careful quantification of the gain consequent on increasing the complexity of the beam delivery. A proposal has been made for an index of beam modulation in terms of the power under the leading part of the spectrum of adjacent bixel fluence changes. It has been shown that as the complexity of the technique increases so the value of this integral modulation index increases and so the dose conformality increases. However, there is no single monotonic relationship found between the dose conformality and the value of this measure of beam conformality. Provided the conditions remain constant, the increase in the value of the integral modulation index leads to an increase in conformality. However, as soon as the planning geometry and/or the importance factors and/or the dose

prescription are changed, the position of the curve in the conformality–beam complexity diagram changes. This indicates that each problem requires a separate investigation. The tools for such an investigation are proposed.

The methodology has been kept deliberately simple since the main goal was to introduce the idea of using a modulation index to describe conformality under differing planning conditions. In this sense figure 8 is the key one. The actual numerical results would change a little if the beam model were divergent, refined to include scatter and if full 3D cases were linked to 2D modulations. A study of clinical cases would also yield plots such as figure 8 but possibly with different gradients. However, it is believed that the fundamental observation would hold of *a quantifiable link between beamspace modulation and conformality which is not universal but problem dependent*.

It is emphasized that this study does not set out to establish the optimum set of segments for fsIMRT. It selects a well-known approach that has been used at this centre (Webb 1991), at Memorial Sloan Kettering Cancer Institute (Mohan *et al* 1992) and at Netherlands Cancer Institute (Bos *et al* 1999). It uses this as a planning approach intermediate between IMRT and CRT. The issue of the optimum number of segments is an area of active research (see, e.g., Bednarz *et al* 2002, Chen *et al* 2001, Cho and Marks 2000, De Gersem *et al* 2001a, 2001b, Shepard *et al* 2002, Xiao *et al* 2000, 2003). It is also emphasized that whilst inverse planning has been used on all the illustrative examples here, forward planning is being actively and successfully pursued by these and other authors for forms of fsIMRT including direct aperture optimization. The methodology in this paper of quantitating conformality against beam modulation index could be extended to many- (rather than two-) segment IMRT.

It should also be commented that CRT with open beams can be improved upon by the use of wedges in some or all beams. This too has not been studied here because the principal goal was to introduce a methodology for comparing planning approaches with two illustrations and to show that no universal, problem-independent, link exists between MI and conformality. It would be expected that if a CRT plan were made with the use of wedges, this would lead to an additional 'point' on the conformality–MI diagram (such as figure 8) for that problem and for that particular planning approach.

Ideally one would like to have a 'universal theory' linking beam modulation to prescribed dose conformality. The author's view is that whilst there have been many useful commentaries on the illconditioning and near-degeneracy of the inverse planning problem (see, e.g., Alber *et al* 2002) there is, as yet, no satisfactory analytic theory giving the 'recipe' for the above link.

The clinical significance of the study is that (at least in the UK) as IMRT becomes established clinically, it is consuming human resources that are in excess of those arranged to service 'conventional' radiotherapy. At least at present, there is also no mechanism in the UK for billing extra (and thus for possibly hiring more staff, always assuming they could be found—not trivial when there are world shortages of radiographers and medical physicists). Hence in rolling out clinical trials of IMRT to many centres, questions are being asked about whether fsIMRT could reasonably substitute for full bixel-modulated IMRT given the latter may require less planning time and less verification effort. The 'yes/no' decision needs to be a clinical judgement of the change in conformality and this demands thorough experience of assessing comparative plans and possibly predicting biological response with models. The purpose of this paper was to show that the loss (or otherwise) of conformality when moving from IMRT to fsIMRT is problem dependent and at present no universal theory exists to help us. The paper gives a methodology for answering the question in specific circumstances.

Acknowledgments

The work of the Joint Department of Physics is supported by Cancer Research UK. I am grateful to Dr Phil Evans and Ms Catherine Coolens for discussion of the topic and for comments on this paper. The referees are thanked for suggestions which have improved this paper.

References

Alber M, Meedt G, Nüsslin F and Reemtsen R 2002 On the degeneracy of the IMRT optimisation problem *Med. Phys.* **29** 2584–9

Bednarz G, Michalski D, Houser C, Huq M S, Xiao Y, Anne P R and Galvin J 2002 The use of mixed-integer programming for inverse treatment planning with pre-defined field segments *Phys. Med. Biol.* **47** 2235–45

Bortfeld T R, Kahler D L, Waldron T J and Boyer A L 1994 X-ray field compensation with multileaf collimators *Int. J. Radiat. Oncol. Biol. Phys.* **28** 723–30

Bortfeld T and Schlegel W 1993 Optimization of beam orientations in radiation therapy: some theoretical considerations *Phys. Med. Biol.* **38** 291–304

Bos L J, van der Horst A, Brugmans M J P, Damen E M F, Mijnheer B J and Lebesque J V 1999 Optimisation of segmented intensity-modulated radiotherapy of prostate cancer *Radiother. Oncol.* **51** (Suppl 1) S6

Chen Y, Michalski D, Xiao Y and Galvin J M 2001 Automatic aperture selection and IMRT plan optimization by beam weight renormalization *Int. J. Radiat. Oncol. Biol. Phys.* **51** (Suppl 1) 74

Cho P S and Marks II R J 2000 Hardware-sensitive optimization for intensity modulated radiotherapy *Phys. Med. Biol.* **45** 429–40

Coolens C, Webb S, Evans P M and Seco J 2003 Combinational use of conformal and intensity-modulated beams in radiotherapy planning *Phys. Med. Biol.* **48** 1795–1807

De Gersem W, Claus F, de Wagter C and de Neve W 2001a An anatomy-based beam segmentation tool for intensity modulated radiation therapy and its application to head-and-neck cancer *Int. J. Radiat. Oncol. Biol. Phys.* **51** 849–59

De Gersem W, Claus F, de Wagter C, VanDuyse B and de Neve W 2001b Leaf position optimization for step-and-shoot IMRT *Int. J. Radiat. Oncol. Biol. Phys.* **51** 1371–88

Hunt M A, Hsiung C-Y, Spirou S V, Chui C-S, Amols H I and Ling C C 2002 Evaluation of concave dose distributions created using an inverse planning system *Int. J. Radiat. Oncol. Biol. Phys.* **54** 953–62

Llacer J, Solberg T D and Promberger C 2001 Comparative behaviour of the dynamically penalized likelihood algorithm in inverse radiation therapy planning *Phys. Med. Biol.* **46** 2637–63

Mohan R, Mageras G S, Baldwin B, Brewster L J, Kutcher G J, Leibel S, Burman C M, Ling C C and Fuks Z 1992 Clinically relevant optimisation of 3D conformal treatments *Med. Phys.* **19** 933–44

Schulz R J and Kagan 2002 On the role of intensity modulated radiation therapy in radiation oncology *Med. Phys.* **29** 1473–80

Shepard D M, Earl M A, Li X A, Naqvi S and Yu C 2002 Direct aperture optimization: a turnkey solution for step-and-shoot IMRT *Med. Phys.* **29** 1007–18

Shepard D M, Ferris M C, Olivera G H, Reckwerdt P J and Mackie T R 1999 Optimizing the delivery of radiation therapy to cancer patients *SIAM Rev.* **41** 721–44

Webb S 1991 Optimisation by simulated annealing of three-dimensional, conformal treatment planning for radiation fields defined by a multileaf collimator *Phys. Med. Biol.* **36** 1201–26

Webb S 2000 *Intensity Modulated Radiation Therapy* (Bristol: Institute of Physics Publishing)

Webb S 2001 A simple method to control aspects of fluence modulation in IMRT planning *Phys. Med. Biol.* **46** N187–N195

Xiao Y, Censor Y, Michalski D and Galvin J 2003 The least-intensity feasible solution for aperture-based inverse planning in radiation therapy *Ann. Oper. Res.* **119** 183–203

Xiao Y, Galvin J, Hossain M and Valicenti R 2000 An optimized forward-planning technique for intensity modulated radiation therapy *Med. Phys.* **9** 2093–99